

Segmental Dynamics of Bulk Poly(vinyl acetate)- d_3 by Solid-State ^2H NMR: Effect of Small Molecule Plasticizer

Rakesh R. Nambiar[†] and Frank D. Blum^{*,‡}

Departments of Chemistry and Materials Science and Engineering, Missouri University of Science and Technology, Rolla, Missouri 65409-0010

Received July 8, 2008; Revised Manuscript Received October 6, 2008

ABSTRACT: The effect of dipropyleneglycol dibenzoate, a plasticizer, on the glass-transition temperature (T_g) of poly(vinyl acetate) was studied using deuterium solid-state NMR and modulated differential scanning calorimetry (MDSC) from 0 to 20% plasticizer content. Quadrupole-echo ^2H NMR spectra were obtained for methyl deuterated PVAc- d_3 samples with different plasticized amounts. The T_g 's of different plasticized samples were determined from NMR as the temperatures at which the deuterium powder patterns collapsed. It was found that the T_g 's decreased by approximately 6 °C for every 5% increment in the plasticizer content and that the trends in the NMR-determined T_g 's, that is, $T_g(\text{NMR})$, were consistent with those determined by modulated differential scanning calorimetry (MDSC). The $T_g(\text{NMR})$ values were about 36 °C above those of the $T_g(\text{DSC})$ values. This difference in the T_g 's was due to the different time scales of the two experiments which could be accounted for on the basis of time–temperature superposition principles. The experimental NMR line shapes were fitted using a set of simulated spectra generated from the MXQET simulation program. The spectra were based on a model of nearest-neighbor jumps on a truncated icosahedron (soccer ball). The resulting average correlation times were also found to fit a time–temperature superposition with the same parameter. While the T_g was decreased by the amount of plasticizer, it was found that the breadth of the transitions from either the NMR line shapes or the MDSC thermograms did not seem to change much with the amount of added plasticizer.

Introduction

Many polymeric materials contain plasticizers to tailor their physical properties and to meet particular technical needs like flexibility, softness, workability, and pliability. Plasticization is a process in which the glass-transition temperature (T_g) of a polymer is reduced by the addition of molecules generally known as plasticizers.¹ In a polymer–plasticizer system, polymer segments experience a local environment containing chain segments and plasticizer units.² Because of a decrease in the local monomeric friction coefficient, segments near several plasticizer molecules may experience increased levels of mobility that result in the reduction of relaxation times and T_g 's. Several theories have been developed to account for the observed characteristics of the plasticization process. Sears and Darby³ have reviewed the theoretical treatment of plasticization in which they describe three primary theories, namely, the lubricating theory, gel theory, and free volume theory. The free volume theory, which is widely accepted, proposes that when small plasticizer molecules are added, they can expand the total free volume in a polymer matrix thereby making it possible for longer-range segmental motions to occur at reduced temperatures.⁴

In addition to theoretical work, there are numerous experimental investigations of the effect of plasticizers on the physical properties of polymers.^{5–9} Various techniques like dielectric spectroscopy,¹⁰ fluorescence correlation spectroscopy,¹¹ photon correlation spectroscopy,¹² dynamic mechanical analysis,¹³ and nuclear magnetic resonance spectroscopy (NMR)^{14–20} have been used to study the effect of plasticizers in a polymer–plasticizer system. These studies have led to the conclusion that many factors influence the T_g depression in a polymer–plasticizer system. Generally, these factors include the rigidity of the polymer; the mobility concentration, size, and flexibility of the

plasticizer; and the interaction between the polymer and plasticizer.

Nuclear magnetic resonance is especially useful for conducting studies near the glass transition. The analysis of the nuclear magnetic resonance line shapes and relaxation times is well established, and recent advances have extended the dynamic range in solids to slow and even ultraslow motions. In favorable cases, experiments can yield specific information about the types of molecular reorientation processes involved.^{21–24} However, only a few of these studies have been extended to polymer–plasticizer systems. Garnaik and Sivaram¹⁶ used ^{13}C CP/MAS NMR to study the effect of polymer–plasticizer interaction for poly(vinyl chloride) containing dioctylphthalate indicating the presence of a hydrogen-bonding interaction. Ganapathy et al.¹⁵ explored the effect of water on poly(vinyl acetate). The use of isotopes and other nuclei allows the separate measurement of polymer or diluents. Blum et al.²⁵ used a combination of high-resolution ^{13}C NMR, ^2H NMR, and electron spin resonance (ESR) to probe the effects of different types of solvents which act as diluents on the polymer dynamics. Kambour et al.⁶ have used ^{31}P NMR of trioctylphosphate in polymer blends to show that the plasticizer resonance narrowed just below the T_g for the system. More recently, Bingemann et al.²⁰ have probed the behavior of both poly(methyl methacrylate)- d_3 and tri-*m*-cresyl phosphate (TCP) with both ^2H and ^{31}P NMR. For a 50% (w/w) blend of the polymer and plasticizer, they found, among other things, that the plasticizer resonance narrows at temperatures well below the temperature where the polymer resonance narrows.

Poly(vinyl acetate) (PVAc) is an important polymer that can be used in many applications because of its bulk and surface characteristics. PVAc has a relatively low T_g , which is important for processing and use of the polymer in applications such as paints, adhesives, thin films, and surface coatings. PVAc can also be easily plasticized, which significantly broadens its range of applications. The molecular mass characterization data for the polymers used is shown in Table 1.

* To whom correspondence should be addressed. Phone: (573) 341-4451. Fax: (573) 341-6033. E-mail: fblum@mst.edu.

[†] Current address: School of Chemistry and Biochemistry, Georgia Institute of Technology, Atlanta, GA, 30332.

[‡] Formerly: University of Missouri-Rolla.

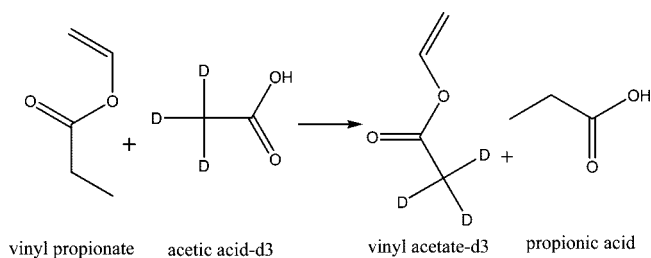
Table 1. Molecular Mass and Polydispersity of the Polymer Samples

sample	molecular mass (kg/mol)	polydispersity
protonated PVAc	240	2.0
deuterated PVAc	236	2.2

In the present paper, we report studies of PVAc plasticized with dipropylene glycol dibenzoate (DPGDB). ^2H NMR of PVAc- d_3 has been used to probe the dynamics of the polymer as a function of plasticizer content through the glass-transition region. This study builds on our previous studies on PVAc- d_3 ^{25,26} and also on poly(methyl acrylate) (PMA)^{27–29} in bulk and on silica surfaces using solid-state deuterium NMR. These prior NMR studies have also been correlated with the results of differential scanning calorimetry (DSC)^{30–32} measurements. The purpose of this work is to determine the T_g 's of the system as a function of plasticizer, to probe the relationships between the NMR and DSC experiments on a plasticized system, and to compare the transition behavior for different compositions. The correlation times for the side chain methyl-group motions are also estimated from the line shapes by modeling them on a jump model based on the geometry of a truncated icosahedron (soccer ball).

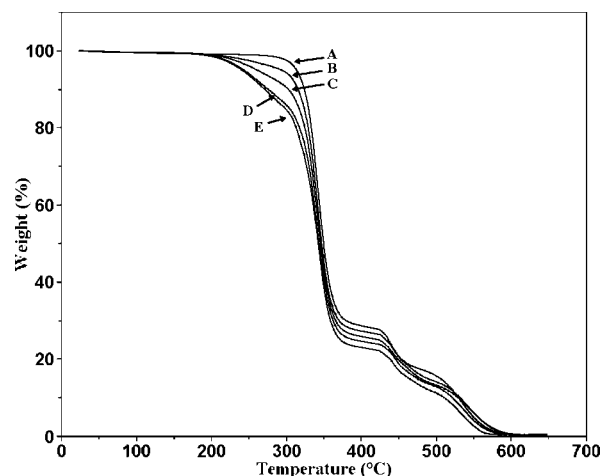
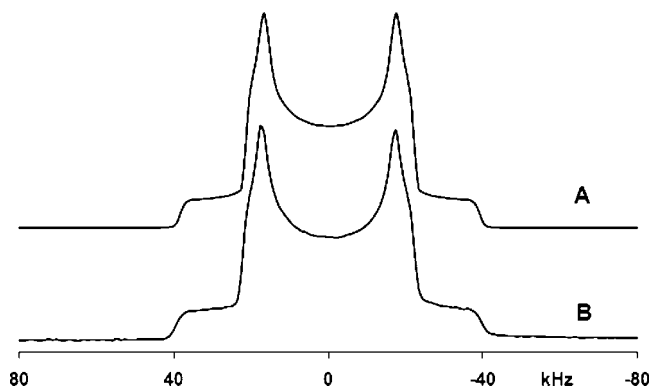
Experimental Section

Synthesis of Deuterated Monomer. Vinyl acetate- d_3 was prepared via an interchange reaction of acetic acid- d_3 and vinyl propionate.²⁶ A mixture of 0.167 mol of acetic acid- d_3 (Aldrich, Milwaukee, WI), 0.33 mol of vinyl propionate (Lancaster Synthesis Inc., Windham, NH), 4.01 mmol of mercuric acetate (Aldrich), 0.42 mmol of concentrated sulfuric acid (98%, Fisher, Pittsburgh, PA), and a trace amount of hydroquinone (Eastman Kodak Co., Rochester, NY) were stirred in three neck flasks at 85–90 °C for 3–4 h. The completion of the reaction was monitored by solution-state ^1H NMR. About 6.68 mmol of sodium acetate was added after the reaction appeared to be complete, and the resultant vinyl acetate- d_3 was collected by distillation under reduced pressure. The product was then purified using a spinning band column. The yield was about 45% on the basis of the amount of acetic acid used. The reaction scheme is shown below.



Synthesis of Deuterated Polymer. Vinyl acetate- d_3 was polymerized in a $\text{K}_2\text{S}_2\text{O}_8$ /sodium-dodecyl sulfate/water emulsion. Deuterated vinyl acetate- d_3 (3.5 g), double-distilled water (3.4 g), $\text{K}_2\text{S}_2\text{O}_8$ (3 mg), and sodium dodecylsulfate (7 mg) were mixed in a flask and were flushed for about 5–10 min with nitrogen gas. Emulsion polymerization was carried out at 70 °C for about 3–4 h using a magnetic bar for stirring. The yield of polymer was approximately 70% on the basis of the amount of monomer used. A protonated polymer, with a molecular mass similar to the deuterated one, was purchased from Scientific Polymer Products (Ontario, NY).

Molecular Mass Determination. Molecular masses were measured using gel permeation chromatography (GPC) in tetrahydrofuran (THF) with an Optilab DSP differential refractometer (Wyatt Technology, Santa Barbara, CA) and a DAWN EOS light-scattering instrument (Wyatt Technology, Santa Barbara, CA) at 690 nm attached to a gel permeation chromatography instrument. Measure-

**Figure 1.** Thermogravimetric (TGA) analysis for (A) 0%, (B) 5%, (C) 10%, (D) 15%, and (E) 20% plasticized PVAc samples.**Figure 2.** Simulated (A) and experimental (B) deuterium NMR spectra of bulk PVAc at 40 °C. The simulated spectrum is based on a truncated icosahedron (soccer ball) and an asymmetry parameter.

ments were made at room temperature using THF as a solvent with a flow rate of 0.5 mL/min. The dn/dc value was taken as 0.057.³³

Preparation of Bulk Plasticized Samples. Plasticized samples containing PVAc and dipropylene glycol dibenzoate (DPGDB, Aldrich) were prepared from thin films. DPGDB has a glass transition of −53 °C.³⁴ Solutions of PVAc- d_3 (or PVAc) in acetone were prepared by mechanical shaking for 2–3 h. These solutions were cast on clean glass slides and were allowed to dry for 24 h. Samples prepared in this way were found to be homogeneous. The thin films seemed to have uniform distributions of the DPGDB in the polymer as evidenced by relatively narrow T_g 's in MDSC thermograms. In contrast, samples prepared by evaporating acetone from bulklike samples did not appear to have uniform distributions of plasticizer. Samples with 0% (no plasticizer used), 5%, 10%, 15%, and 20% plasticizer were prepared.

Characterization of the Samples by TGA and MDSC. The amounts of polymer and plasticizer present were verified by thermogravimetric analysis (TGA) (TA Instruments, New Castle, DE). The scans were run at a heating rate of 10 °C/min in air. The thermal behavior in the glass-transition region was measured with a TA Instruments Model 2920 MDSC (New Castle, DE). An empty pan was used as the reference in the MDSC experiments. Two heating scans and one cooling scan were taken from −40 to 150 °C, at a rate of 2.5 °C/min, a modulation amplitude of ± 0.5 °C, and a period of 60 s. The mass of the samples used was approximately 8–12 mg, and the cell was purged with nitrogen gas at 50 mL/min during the scans. The second heating scan was used to determine the T_g data for the reversing heat flow curves so that all of the samples were subjected to a similar thermal history. The results are shown as differential reversing heat flow (dQ_{rev}/dT) versus temperature (T). The reported T_g was determined as the

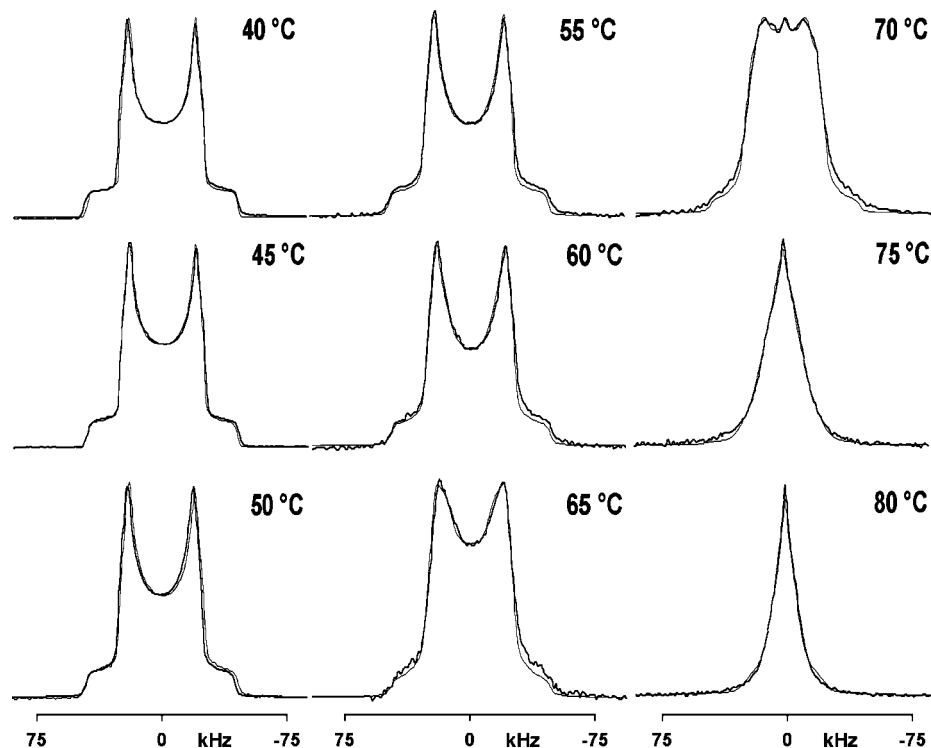


Figure 3. Experimental (black) and simulated (gray) ^2H NMR spectra for bulk PVAc- d_3 as a function of temperature.

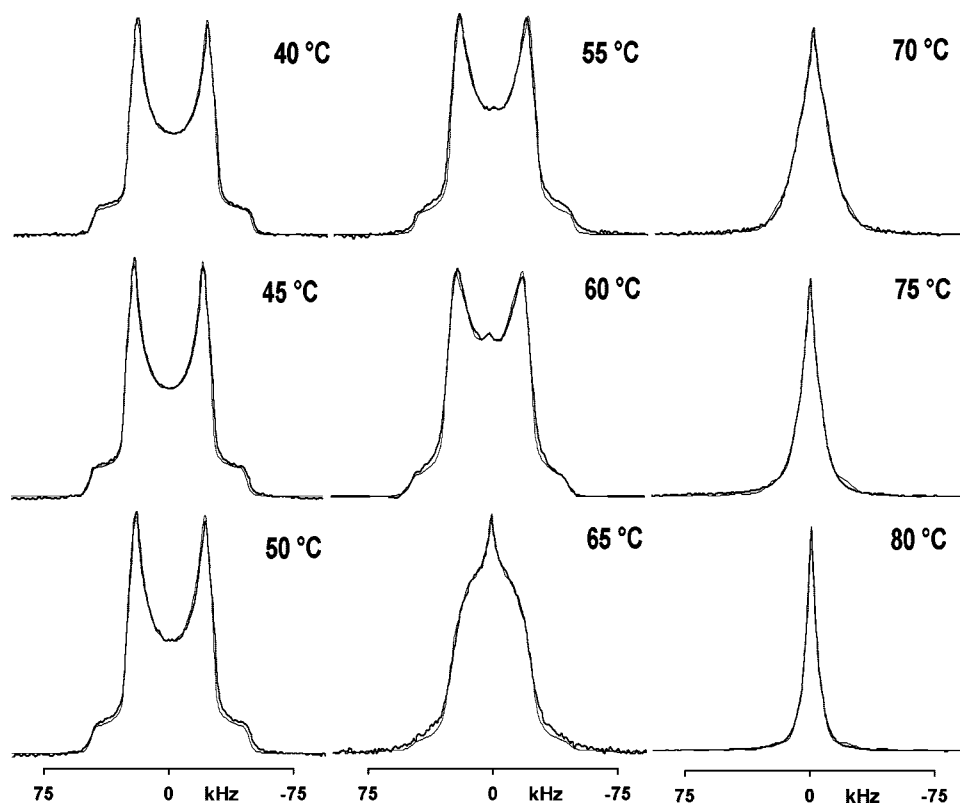


Figure 4. Experimental (black) and simulated (gray) ^2H NMR spectra for bulk 5% plasticized PVAc- d_3 as a function of temperature.

temperature at which the derivative of the reversing heat flow versus temperature was at a maximum.

Characterization of the Samples by Solid-State ^2H NMR. The NMR spectra were obtained using a Varian VXR-400/S spectrometer equipped with a fixed-frequency wide-line probe (Doty Scientific, Columbia, SC), a high-power amplifier, and a fast digitizer. The wide-line probe had a coil that could accommodate an 8 mm (diameter) sample. The quadrupole-echo pulse sequence

(delay- 90_y - τ - 90_x - τ -acquisition) was used with a ^2H frequency at 61.39 MHz. The 90° pulse width was $2.8 \mu\text{s}$ and an echo time (τ) of $30 \mu\text{s}$ was used. The Fourier transform was started from the top of the echo, and no line broadening was applied to the spectra. The number of scans collected for bulk samples ranged from 700 to 1000 depending on the temperature of operation. The spectra were taken at intervals of 5°C from 40 to 80°C . The spectra were processed using the Mestrec software package (Santiago de

Compostela University, Spain), and each spectrum shown was scaled to the same height for easier comparison. The reported T_g (NMR) was the temperature at which the powder pattern collapsed to form a single peak.

Simulation Studies of the Experimental Spectra. The experimental NMR line shapes were simulated using a FORTRAN program known as MXQET.^{35,36} The simulation was based on a truncated icosahedron (soccer ball).³⁷ The vertices were defined as the jump sites (60 sites) for the symmetry axis of the methyl group (effective C–D bond vector). Different geometric models like tetrahedron (4 sites), octahedron (6 sites), and dodecahedron (20 sites) were also studied with the simulation program.³⁷ Of these models, the soccer ball model provided a set of line shapes that were close to those of the experimental ones, probably because the model came reasonably close to a small jump model. Additional information about the simulation can be found elsewhere.³⁷ A reduced quadrupole-coupling constant of 59 kHz was used in the simulations to account for the fast methyl group rotation around the symmetry axis. The pulse spacing was 30 μ s while a pulse width of 2.8 μ s was used for the quadrupole-echo pulse sequence in the simulations. To account for the asymmetric behavior of the line shapes for poly(vinyl acetate)²⁶ (vide infra), an asymmetry parameter of 0.12 was used with a slight Gaussian broadening of 0.1 kHz. A series of simulated line shapes with different jump rates were produced using the simulation program. The experimental line shapes were then fitted to a superposition of simulated spectra by using a mathematical routine (MATLAB, The Mathworks, Inc., Natick, MA). The weighting factors of each of the simulated spectra were found by solving a system of linear equations. A constrained least-squares fit was applied to find the positive weighting factors of a series of spectra.

Results

The amount of the plasticizer present in the samples was verified using thermogravimetric analysis (TGA). The decomposition thermograms for the bulk and plasticized samples are shown in Figure 1. Above 500 °C, the thermogram for the bulk PVAc is slightly different from those for the other samples. The plasticizer decomposes in the range of 290–325 °C. The upper range of this decomposition (from 325 to 375 °C) is where the major mass loss for the polymer occurs. Using either the region of the thermogram between 290 and 325 °C or between 375 and 425 °C yielded estimates of the plasticizer amounts that are within experimental error ($\pm 0.5\%$ absolute) of the values on the basis of the composition of the original (nominal) solution.

The experimental and simulated ^2H NMR spectra of the bulk (0% plasticized) PVAc- d_3 at 40 °C are shown in Figure 2. The experimental spectrum consisted of a powder pattern with a splitting of 35 kHz at the high points (horns) and, although the horns did not drop sharply on the outsides, the spectral separation was about 44 kHz at their base. The simulation was based on a reduced quadrupole-coupling constant (QCC) of 59 kHz and 0.1 kHz Gaussian broadening. This reduction occurred because of the fast rotational motion of the methyl group about its symmetry axis, which effectively decoupled the methyl rotation from the backbone motions. To account for the bumps rising from the shoulders,²⁶ the simulation also included a small asymmetry parameter ($\eta = 0.12$). The simulated spectrum was based on the nearest-neighbor jumps of a truncated icosahedron (soccer ball, 60 sites) for the symmetry axis of the methyl group.

Quadrupole echo ^2H NMR spectra for bulk PVAc- d_3 were taken as a function of temperature and plasticizer amount. The resulting experimental and simulated spectra are shown in Figures 3–7. Each of the spectra for each group was normalized to a constant height. The spectra at lower temperatures, for the 0% plasticized (bulk) PVAc sample (shown in Figure 3), were indicative of the Pake powder pattern as discussed above. At low temperatures, the backbone motions of the polymer were

slow on the deuterium NMR time scale. As the temperature was increased from 40 to 80 °C, the powder pattern collapsed from a Pake powder pattern at 40 °C, through a hump-shaped feature at 70 °C, with a gradual smoothing of the sharp features, to a single narrower resonance at 80 °C. It is easy to observe the spectra go from a Pake pattern (glass) to a relatively narrow isotropic resonance (rubber) with increased temperature. Defining a T_g (NMR) is a little more complicated. Consistent with earlier protocol,²⁶ we define the T_g (NMR) in the middle of the range where the spectra go from a powder pattern to a single resonance. More specifically, we assign a single value for the T_g (NMR) as the temperature where the “horns” of the Pake pattern are no longer distinguishable as “peaks”. For example, in Figure 3, this would be expected around 71 °C for the bulk sample. This compares with around 69 °C for a similar PVAc from prior studies.²⁶ The uncertainties of the estimation of the collapse and the temperature (systematic) of the sample are expected to be less than ± 3 °C.

The ^2H NMR spectra for the 5% plasticized sample of bulk PVAc are shown in Figure 4 as a function of temperature. Spectral line shape changes, similar to those for the bulk sample, were observed except that the collapse of the powder pattern occurred at lower temperatures. The NMR glass transition takes place roughly between 60 and 65 °C and is centered at T_g (NMR) ~ 63 °C.

The spectra for the 10% plasticized PVAc- d_3 sample are shown in Figure 5. These spectra are also similar in form to those of the other samples including a shift to higher mobility at the same temperatures. The spectra collapsed to a broad resonance between 55 and 60 °C with the T_g (NMR) assigned to 58 °C for this sample.

The spectra for the 15% and 20% plasticized samples are shown in Figures 6 and 7, respectively. These spectra also show that the polymer mobility is greater at lower temperatures than it is in the samples with less plasticizer. The collapse of the powder pattern took place within a range of 50–55 °C or T_g (NMR) ~ 52 °C for the 15% plasticized sample. The T_g (NMR) for the 20% plasticized sample can be assigned as 48 °C on the basis of the collapse occurring between 45 and 50 °C.

The simulations of the experimental ^2H NMR spectra are shown superimposed as lighter lines in Figures 3–7. The fits seemed to be quite good, in most cases, and are generally coincidental with the experimental spectra. The simulated spectra were based on a series of component spectra with jump rates from 100 Hz to 1.0×10^{11} Hz. A system of linear equations was fit using MATLAB to match the experimental spectra. Bar graphs of the distributions of component spectra as a function of temperature and plasticizer content are given in the Supporting Information. For simplicity, the jump rates from the component spectra can be divided into three groups or regimes with respect to their powder pattern intensities, namely, slow, intermediate, and fast. The group of exchange rates with powder patterns that did not result in significant intensity loss during quadrupole echo was identified as the slow regime (10^2 – 10^4 Hz). The intermediate motion regime (10^4 – 10^6 Hz) was classified as the region where the exchange rates resulted in significant loss of intensity.³⁸ Finally, the fast regime, about 10^6 – 10^{11} Hz, on the fast side of the intensity versus jump rate curve, resulted in echoes with little intensity loss. The fractions of each component of the motional regimes used in the fittings at different temperatures are given in Table 2. On the basis of the analysis above, it is noted that the line-shape criterion used to estimate the T_g (NMR) roughly corresponds to where only 5% of the slow component contributes to the simulated spectrum.

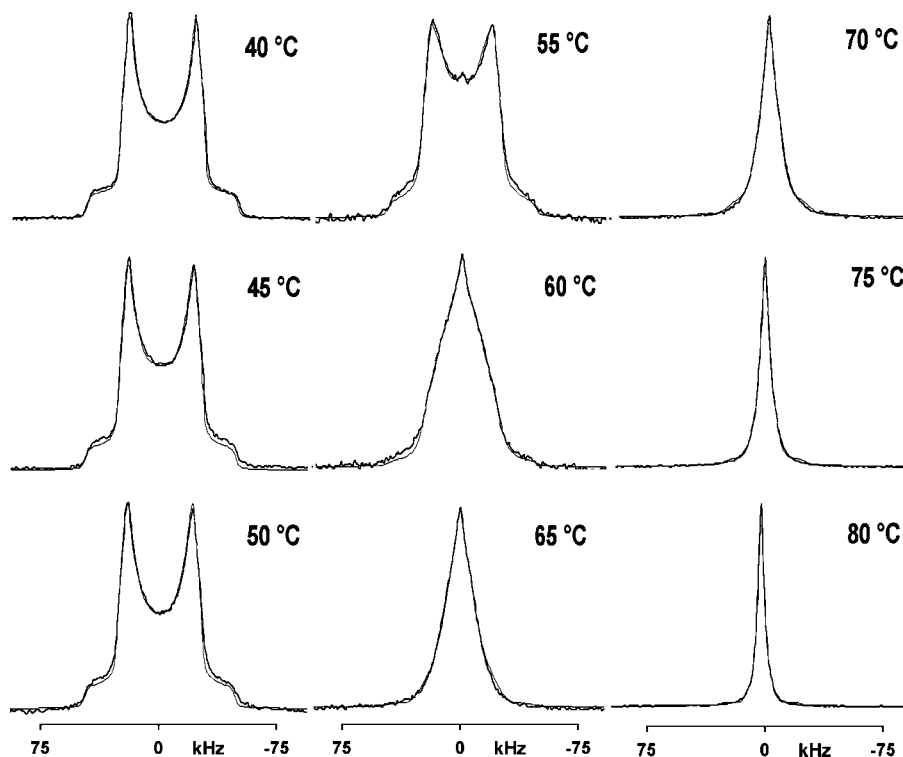


Figure 5. Experimental (black) and simulated (gray) ^2H NMR spectra for bulk 10% plasticized PVAc- d_3 as a function of temperature.

The time correlation functions for each of the basis set spectra were calculated by the MSQET program for our jump model.³⁶ Good fits required a broad distribution of spectra with widely different jump rates covering about 5 orders of magnitude in jump rate. While the sensitivity to contributions in the extremes of the distribution was low, the fitted results give a good sense of breadth of the distribution. For each experimental spectrum, the superposition of the correlation functions for the component

spectra formed a master correlation function. These master time correlation functions were integrated to yield an average correlation time or $\langle\tau_c\rangle$.³⁹ The average correlation times were calculated and plotted as a function of temperature and plasticizer content in the Supporting Information. However, with a broad distribution of jump rates (or correlation times), $\langle\tau_c\rangle$ was dominated by the long correlation times. A more representative set of values is the weighted average of the logarithm

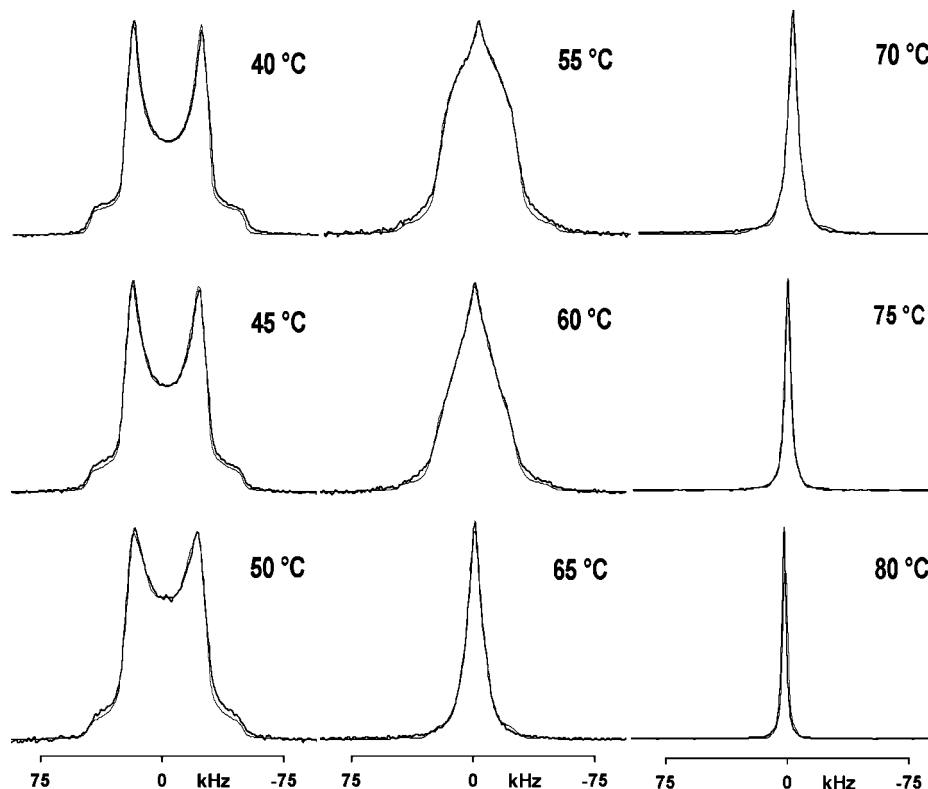


Figure 6. Experimental (black) and simulated (gray) ^2H NMR spectra for bulk 15% plasticized PVAc- d_3 as a function of temperature.

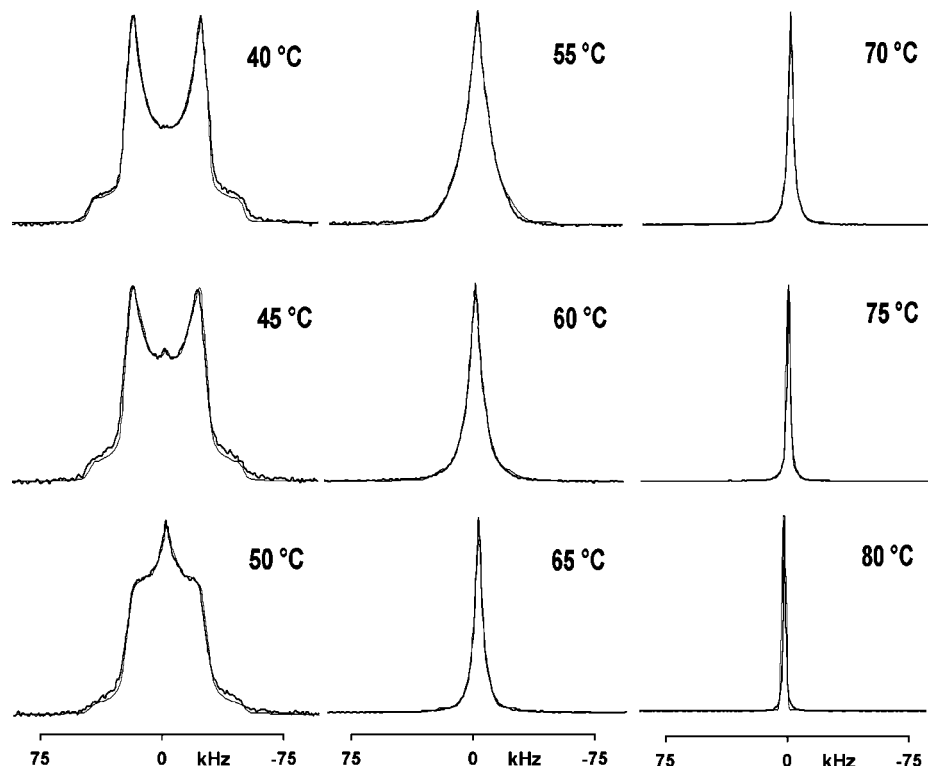


Figure 7. Experimental (black) and simulated (gray) ^2H NMR spectra for bulk 20% plasticized PVAc- d_3 as a function of temperature.

Table 2. Motional Components Used To Simulate Experimental Line Shapes^{a,b}

	0% plast.			5% plast.			10% plast.			15% plast.			20% plast.		
$T(^{\circ}\text{C})$	S	I	F	S	I	F	S	I	F	S	I	F	S	I	F
40	91	9		100			42	58		46	54		36	64	^c
45	45	55		50	50		30	70		17	83		4	96	^c
50	41	59		33	67		30	70		7	93		4	96	^c
55	43	57		14	86		7	93	^c	2	98	^c		99	1
60	25	75		10	90	^c	1	99	^c	1	99	^c		99	1
65	7	93		2	97	^c		100	^c		100	^c		96	4
70	3	97	^c		100	^c		99	1		100	^c		92	8
75		100	^c		99	1		99	1		91	9		73	27
80		100	^c		98	2		95	5		80	20			100

^a Components: S, slow ($k \leq 1.0 \times 10^4$ Hz); I, intermediate ($1.0 \times 10^4 < k \leq 1.0 \times 10^6$ Hz); F, fast ($1.0 \times 10^6 < k \leq 1.0 \times 10^{11}$ Hz) where k is the jump rate. ^b Given as the percentages of each component in the simulated spectra. ^c A small (<1%) but nonzero component was required for a good fit.

of the jump rate, $\langle \log k \rangle$. These are plotted in Figure 8 as a function of temperature and plasticizer content. The $\langle \log k \rangle$ values varied with temperature in an Arrhenius manner with apparent energies of activation of 83–108 kJ/mol.

Thermal analyses of the samples were performed using modulated differential scanning calorimetry (MDSC). The thermograms for PVAc samples are shown in Figure 9. The derivative of the reversible heat flow was plotted as a function of temperature for the different plasticized PVAc samples. The maximum of the derivative reversible heat flow curve was chosen as the T_g (DSC). The maxima, T_g 's, were shifted to lower temperatures as the amount of plasticizer increased averaging 6.5 degrees for every 5% plasticizer added. All of the samples had similar glass-transition widths (10–13 $^{\circ}\text{C}$ from the half-width at half-height). The existence of a single relatively sharp transition curve obtained during the MDSC experiments indicated that the polymer–plasticizer system is miscible and that to a first approximation no evidence of microphase separation was observed.

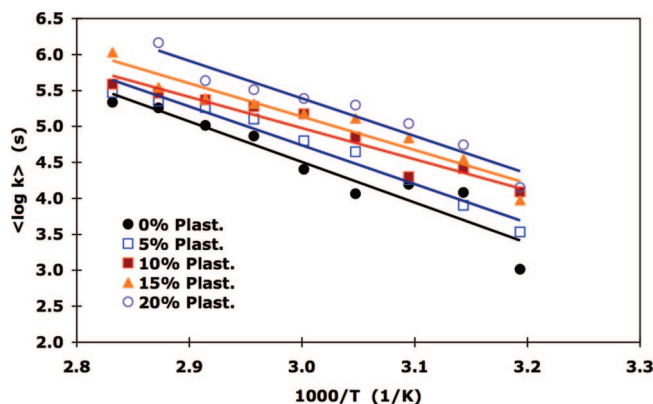


Figure 8. Averages of the log jump rates values, $\langle \log k \rangle$, as a function of temperature for the different plasticized (0, 5, 10, 15, 20% plasticizer) samples.

Discussion

For the ^2H NMR spectra of PVAc- d_3 at lower temperatures, a Pake powder pattern was observed. For a ^2H nucleus (nuclear spin quantum number, $I = 1$), the quadrupolar splitting $\Delta\nu_q$ is given by³⁸

$$\Delta\nu_q = (3/4)(e^2qQ/h)(3 \cos^2 \theta(t) - 1 - \eta \sin^2 \theta(t) \cos^2 \phi(t)) \quad (1)$$

where e^2qQ/h is the quadrupole coupling constant, θ and ϕ are spherical polar angles for the orientation of the principle axis system of the electric-field tensor relative to the applied static magnetic field, \mathbf{B}_0 , and η is the asymmetry parameter of the quadrupolar tensor. In general, the spherical polar angles vary with time, t . For a C–D bond or a methyl group in particular, the $3 \cos^2 \theta(t) - 1$ term can be expanded to

$$\langle 3 \cos^2 \theta(t) - 1 \rangle = (1/2) \langle 3 \cos^2 \delta(t) - 1 \rangle \langle 3 \cos^2 \chi(t) - 1 \rangle \quad (2)$$

where $\langle \rangle$ represents the time average, $\delta(t)$ is the angle between the \mathbf{B}_0 and the rotation axis, and χ is the angle between the

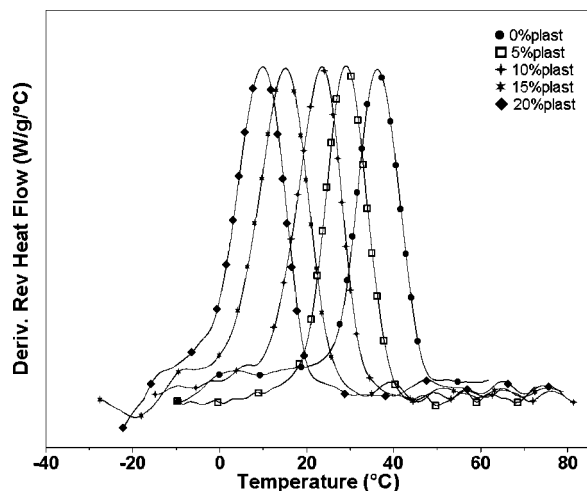


Figure 9. MDSC derivative heat flow curves for different plasticized samples of bulk PVAc. The maximum of the derivative curve is taken as the T_g (DSC) reported.

rotation axis and the C–D bond. Since χ is 70.5° for a methyl deuteron, the $3 \cos^2 \chi - 1$ term is reduced and the quadrupolar splitting is reduced to 1/3 of its original value. Full values for QCC of the methyl groups are typically about 150–170 kHz.⁴⁰

The line shapes for PVAc- d_3 at lower temperatures (e.g., Figure 2), especially the existence of the curved shoulders, were similar to the line shapes found in other samples²⁶ like L-alanine,^{41,42} thymine- d_3 ,⁴³ and [1,1,1,3,5,6- d_6]-*n*-butyl 2,4,6-octatrienyllideneimine.⁴⁴ The presence of the shoulders can be modeled by using a nonzero asymmetry parameter. For methyl-group rotation in acetates, deuterons experience a nonuniform field because of the presence of the nearby carbonyl oxygen that distorts the C–D bond. Acrylates and related compounds do not show this effect because the carbonyl oxygen is separated from the methyl group by another oxygen atom resulting in no such distortion of the bond angle. Like thymine- d_3 ,⁴³ the deuteron closest to the carbonyl oxygen in PVAc- d_3 experienced a change in both the QCC and η compared to the other two deuterons on the methyl group.

At 40 °C, all of the PVAc- d_3 samples exhibited a Pake powder pattern with an effective QCC of 59 kHz. The Pake powder patterns (slow motional regime) for PVAc- d_3 collapsed to motionally narrowed resonances (fast motional regime) with increasing temperature because of the changes in the segmental mobility of the polymer. The temperature at which the powder pattern collapses to a single (broad) resonance can be considered as the glass-transition temperature for the deuterium NMR experiment, that is, T_g (NMR). The T_g (NMR) for the bulk PVAc sample was about 71 °C which is close to the T_g (67 °C) observed for PVAc- d_3 in our previous work.²⁶ The intensity of the central component at a given temperature increased with increases in the plasticizer content consistent with an increase in the mobility of the polymer segments. Before the Pake powder pattern collapsed into a motionally narrowed resonance, the line shapes of all of the samples passed through a hump-shaped feature. The hump-line shape can be considered as a superposition of residual powder patterns and a motionally narrowed mobile component. Near the T_g (NMR), a small amount of a central component is observed before most of the powder pattern collapses. This small amount of material is believed to be due to segments near the chain ends that have additional mobility.³⁷

As previously mentioned, the intensity of the middle (motionally narrowed) component, at a given temperature, increased as a function of plasticizer content. Hence, through fitting of the spectra, the motional enhancement due to the plasticizer can be quantified. As the temperature increased, the polymer

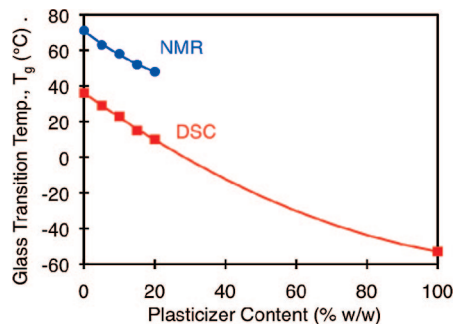


Figure 10. Glass-transition temperatures (T_g 's) as a function of plasticizer content in PVAc (wt %) from both DSC and NMR. The DSC curve is fitted to eq 4 with $b = -0.60$.

segments underwent faster segmental motions. It has been proposed that the plasticizer increases the amount of free volume and allows long-range segmental motions to take place, thus providing greater mobility to the chains with higher plasticizer content. It has also been postulated that the plasticizers occupy the free volume of the host polymer interrupting the polymer–polymer interactions in favor of polymer–plasticizer ones.⁴⁵

The jump-rate distributions from the simulations of the ^2H spectra yield information about the homogeneity of the segmental motions in the samples. While more accurate estimates of the segmental motion of the polymer are available from, for example, two- and higher-dimensional studies,^{20,24,39,46} our approach captures the nature of the breadth of the distributions of segmental motions. The jump rates have been divided into three parts, namely, rigid, intermediate, and fast. At lower temperatures, the distribution of jump rates is broad ranging from rigid to intermediate with small amounts from a faster regime. There appeared to be a trend toward homogeneity of the segmental motions as we approached the glass-transition region after which the samples had more homogeneous distributions mainly in the fast jump rate regime. The addition of plasticizer did not appear to change the breadth of the distribution of jump rates. However, we observed that the distribution shifted to faster jump rates at lower temperatures as compared to the samples with lesser plasticizer content.

The line shapes are reasonably well described by the soccer ball jump model. Two-dimensional NMR on PVAc suggested that the PVAc segments reoriented with about 10° jumps plus rotational diffusion for the α -transition.²⁴ This model is fairly consistent with that used here with our relatively small jumps. The correlation times calculated from the model and shown in Figure 8 were consistent with those expected for deuterium line shape changes. The correlation functions were nonexponential and were fit to a stretched exponential where the width parameter, β , was determined from

$$C(t) = \exp(t/\tau_{\text{kww}})^\beta \quad (3)$$

The fitted width parameters were moderately broad (between 0.2 and 0.4) which is consistent with the broad distribution of spectra required for spectral simulations. The apparent independence of the width of the distribution on the plasticizer amount is consistent with previous studies on dioctylphthalate and poly(cyclohexyl methacrylate).⁴⁷ It is also consistent with the studies of PMMA- d_3 , where the polymer was found to exhibit the same heterogeneity (though different T_g) in bulk and with the addition of 50% tri-*m*-cresyl phosphate. Further evidence of the relative independence of the width of the distribution can be gained from a direct comparison in the spectra themselves. Shifting the spectra for the different samples by 5 °C (the increments for which the spectra were taken) for each increment of 5% DPGDP makes them superimposable

except for some small differences in the T_g region where the spectra change a fair amount with even a degree difference.

The NMR and thermal analysis data were also consistent. A comparison of the T_g 's for the PVAc samples from both experiments are shown in Figure 10 as a function of the plasticizer amount. The uncertainties in the estimation of the T_g 's are on the order of the sizes of the symbols in the figure. The dependence of T_g on the plasticizer amount is fairly linear in the range studied. From the linear portion, the slopes of the plots were -1.02 and -1.32 for the NMR and DSC plots, respectively. The T_g decreased by an average of 5.8 °C for every 5% increment of plasticizer from the NMR experiment, while it decreased by 6.5 °C from the DSC experiments. Given that the T_g for the DPGDB is known (-53 °C),³⁴ the T_g (DSC) can be fitted to the established relationship or

$$T_{g,\text{mix}} = T_{g,\text{polym}}w_{\text{polym}} + T_{g,\text{plast}}w_{\text{plast}} + bw_{\text{polym}}w_{\text{plast}}(T_{g,\text{polym}} - T_{g,\text{plast}}) \quad (4)$$

where the T_g 's are for the pure polymer and plasticizer, the w 's are the mass fractions of either component, and b is a constant that depends on the polymer–plasticizer system.^{48,49} The curve for the DSC data is shown with a best empirical fit with $b = -0.60$. This value is consistent with that found for poly(vinyl chloride) with different plasticizers.⁴⁹

The T_g values obtained by the NMR experiments were calculated to be higher than the T_g values for the DSC experiments by 36 ± 2 °C. This difference in the glass-transition temperatures between the NMR and DSC experiments was also found for methyl-labeled poly(methyl acrylate)- d_3 ³⁷ and poly(methyl methacrylate).⁵⁰ This difference can be attributed to the differences in the time scales of the two experiments with the DSC being on the order of Hertz and the deuterium NMR on the order of kilohertz. McCall⁵¹ and Chartoff et al.⁵² showed how different experimental techniques yielded frequency-dependent T_g values. The changes in the glass-transition temperature with frequency can be estimated using the Williams, Landel, and Ferry (WLF) model or

$$\log(\tau/\tau_0) = -C_1(T - T_0)/(C_2 + T - T_0) \quad (5)$$

A variety of estimations of the WLF constants for PVAc exist. Sasabe and Moynihan⁵³ recalculated the values used by Williams and Ferry⁵⁴ from mechanical data to shift to $T_0 = T_g$. Using their constants of $C_1 = 15.6$ and $C_2 = 46.8$ with $\tau_0 = 100$ s for DSC and $\tau = 25$ μ s for NMR (reciprocal of the frequency between the horns), the WLF model predicts that the T_g (NMR) should be 34 °C higher than T_g (MDSC). This difference is fairly close to the difference in the T_g 's obtained experimentally. The value of C_2 estimated from Ferry's book⁵⁵ by changing the reference temperature to the T_g of the bulk polymer suggests a T_g (NMR) about 42 °C above the T_g (DSC). In any case, the two experiments are in reasonable agreement.

The WLF approach may also be extended to the data shown in Figure 8 for the $\langle \log k \rangle$ data as a function of temperature. Shifting the correlation times through the WLF equation above allows the superposition of all of the correlation time data. A plot of this superposition is shown in the Supporting Information. On the basis of this superposition, the apparent energies of activation were estimated to be 78 – 99 kJ/mol, which is about 8% lower than those estimated from Figure 8.

Several experiments on polymer–plasticizer systems and various techniques were used to study the effects of plasticizer on the segmental motion of polymer chains. For example, Royal and Torkelson⁵⁶ used a fluorescence technique to sense the increase in the mobility of polymer (PVAc) chains caused by the plasticization by water. Their studies found that 0.7% by weight of water was enough to depress the T_g by 5 °C, whereas the larger-size plasticizer used in our case depresses the T_g by

5 °C for a plasticized amount of 5%. This can be explained by the fact that the size and mass (i.e., number of molecules) of the plasticizer play an important part in determining its ability to change the conformation in a polymer matrix. The larger the volume needed for motion to occur, the lower the probability that motion will occur.⁵⁷ Deuterium NMR, ^{13}C NMR, and electron spin resonance have also been useful to test the sensitivity of water and other solvents as a plasticizer.²⁵ Line shapes from all three techniques were found to be sensitive to the presence of diluents. Smith and Moll⁵⁸ also used ^2H NMR to probe the changes in deuterated polymers plasticized by CO_2 . They found that the line shapes were insensitive to the presence of CO_2 , while the relaxation times were indicative of enhanced molecular motion of the polymer.

The use of ^{31}P NMR to probe the behavior of plasticized systems has yielded important results for the mobility of the plasticizer. Kambour et al.⁶ have used ^{31}P NMR to study the diluent motion in glassy plasticized blends. With trioctyl phosphate as the diluent, phosphorus line shapes were observed, which changed from an axially symmetric line shape to a narrow line, as the temperature increased. These experiments demonstrated that the diluent moves around in a glassy matrix. Similar conclusions were made by Bingemann et al.²⁰ who used both one- and two-dimensional ^{31}P NMR of tri-*m*-cresol phosphate with PMMA- d_3 . The phosphate resonance became motionally narrowed at temperatures well below that at which the polymer underwent a glass transition. Similar to the results in this present study, the apparent breadth of the distribution of polymer motions seems relatively constant even though the T_g is lowered. One of the remaining pieces for future work is knowledge of the dynamics of the plasticizer in these systems and its relationship to the T_g 's measured by both techniques.

Conclusions

This work has demonstrated the relationships between the results of ^2H NMR and MDSC for the PVAc-DPGDB system from 0 to 20% (w/w) DPGDB. The T_g 's from both techniques paralleled each other and could be fit with a simple mixture model; the same interaction parameter was used for each set of experimental results. Changes in T_g of around 6 °C per 5% DPGDB for each type of experiment were found. The differences between the NMR and MDSC experiments of about 36 ± 2 °C were attributable to the differences in frequency of the two different experiments. A WLF analysis based on mechanical data was consistent with the magnitude of the T_g differences for the two experiments. The WLF C_2 parameter used also allowed the superposition of the $\langle \log k \rangle$ values as a function of inverse temperature.

The ^2H line shapes were fitted using a superposition of simulated spectra based on the MXQET program which is based on a model of nearest-neighbor jumps on a truncated icosahedron (soccer ball). The complex shape of the resonance of poly(vinyl acetate) was modeled with the inclusion of an asymmetry parameter. The fitted spectra resulted in estimation of the distribution of the motional rates of the polymer segments. The change in the motional rates of the segments, with the addition of small plasticizer molecules, was clearly evident in the distribution of motional rates. Consistent with some prior studies, the width of the distribution of motional rates from the line shapes was relatively constant across the range of plasticizer contents studied.

Acknowledgment. The financial assistance from the National Science Foundation under grant DMR-0706197 is acknowledged. The authors also thank Dr. Burak Metin for his assistance with the modeling and also for useful discussions.

Supporting Information Available: Information including the bar graphs representing the component spectra, the plot of the log of the average correlation times as a function of time, and the temperature superposition of the $\langle \log k \rangle$ as a function of temperature. This material is available free of charge via the Internet at <http://pubs.acs.org>.

References and Notes

- (1) Billmeyer, F. W. *Textbook of Polymer Science*, 3rd ed.; Wiley: New York, 1984.
- (2) Marcilla, A.; Beltran, M. In *Handbook of Plasticizers*; Wypych, G., Ed.; ChemTec Pub.: Toronto, Canada, 2004; pp 107–120.
- (3) Sears, J. K.; Darby, J. R. *The Technology of Plasticizers*; Wiley: New York, 1982.
- (4) Boyer, R. F. In *Encyclopedia of Polymer Science and Engineering*, 1st ed.; Bikales, N. M., Ed.; Wiley Interscience: New York, 1977; Vol. 2 Supplement, pp 745–839.
- (5) Jackson, W. J., Jr.; Caldwell, J. R. *J. Appl. Polym. Sci.* **1967**, *11*, 227–244.
- (6) Kambour, R. P.; Kelly, J. M.; McKinley, B. J.; Cauley, B. J.; Inglefield, P. T.; Jones, A. A. *Macromolecules* **1988**, *21*, 2937–2940.
- (7) Williams, G. *J. Non-Cryst. Solids* **1991**, *131*, 1–12.
- (8) Jones, A. A.; Inglefield, P. T.; Liu, Y.; Cauley, B.; Roy, A. K.; Kambour, R. *Mater. Res. Soc., Symp. Proc.* **1991**, *215*, 109–118.
- (9) Maeda, Y.; Paul, D. R. *J. Polym. Sci., Part B: Polym. Phys.* **1987**, *25*, 981–1003.
- (10) Ngai, K. L.; Roland, C. M. *Macromolecules* **1993**, *26*, 6824–6830.
- (11) Best, A.; Pakula, T.; Fytas, G. *Macromolecules* **2005**, *38*, 4539–4541.
- (12) Fytas, G.; Wang, C. H.; Meier, G.; Fischer, E. W. *Macromolecules* **1985**, *18*, 1492–1496.
- (13) Ma, X.; Sauer, J. A.; Hara, M. *Polymer* **1997**, *38*, 4425–4431.
- (14) Schaefer, J.; Garbow, J. R.; Stejskal, E. O.; Lefelar, J. A. *Macromolecules* **1987**, *20*, 1271–1278.
- (15) Ganapathy, S.; Chacko, V. P.; Bryant, R. G. *Macromolecules* **1986**, *19*, 1021–1029.
- (16) Garnaik, B.; Sivaram, S. *Macromolecules* **1996**, *29*, 185–190.
- (17) Parker, A. A.; Hedrick, D. P.; Ritchey, W. M. *J. Appl. Polym. Sci.* **1992**, *46*, 295–301.
- (18) Parker, A. A.; Hedrick, D. P.; Ritchey, W. M. *Macromolecules* **1992**, *25*, 3365–3368.
- (19) Atsushi, A.; Takegoshi, K. *J. Chem. Phys.* **2001**, *115*, 8665–8669.
- (20) Bingemann, D.; Wirth, N.; Gmeiner, J.; Rossler, E. A. *Macromolecules* **2007**, *40*, 5379–5388.
- (21) Spiess, H. W. *Colloid Polym. Sci.* **1983**, *261*, 193–209.
- (22) Spiess, H. W. *J. Chem. Phys.* **1980**, *72*, 6755–6762.
- (23) Lausch, M.; Spiess, H. W. *J. Magn. Reson.* **1983**, *54*, 466–479.
- (24) Tracht, U.; Heuer, A.; Spiess, H. W. *J. Chem. Phys.* **1999**, *111*, 3720–3727.
- (25) Blum, F. D.; Dickson, J. E.; Miller, W. G. *J. Polym. Sci., Part B: Polym. Phys.* **1984**, *22*, 211–21.
- (26) Blum, F. D.; Xu, G.; Liang, M.; Wade, C. G. *Macromolecules* **1996**, *29*, 8740–8745.
- (27) Lin, W.-Y.; Blum, F. D. *Macromolecules* **1997**, *30*, 5331–5338.
- (28) Lin, W.-Y.; Blum, F. D. *Macromolecules* **1998**, *31*, 4135–4142.
- (29) Lin, W. Y.; Blum, F. D. *J. Am. Chem. Soc.* **2001**, *123*, 2032–2037.
- (30) Porter, C. E.; Blum, F. D. *Macromolecules* **2000**, *33*, 7016–7020.
- (31) Porter, C. E.; Blum, F. D. *Macromolecules* **2002**, *35*, 7448–7452.
- (32) Zhang, B.; Blum, F. D. *Macromolecules* **2003**, *36*, 8522–8527.
- (33) Brandrup, J.; Immergut, E. H. *Polymer Handbook*, 3rd ed.; Wiley: New York, 1989.
- (34) Capaccioli, S.; Prevosto, D.; Lucchesi, M.; Rolla, P. A.; Casalini, R.; Ngai, K. L. *J. Non-Cryst. Solids* **2005**, *351*, 2643–2651.
- (35) Greenfield, M. S.; Ronemus, A. D.; Vold, R. L.; Vold, R. R.; Ellis, P. D.; Raidy, T. E. *J. Magn. Reson.* **1987**, *72*, 89.
- (36) Vold, R. R.; Vold, R. L. *Adv. Magn. Opt. Reson.* **1991**, *16*, 85–171.
- (37) Metin, B.; Blum, F. D. *J. Chem. Phys.* **2006**, *124*, 054908/1–54908/10.
- (38) Abragam, A. *The Principles of Nuclear Magnetism*; Clarendon Press: Oxford, U.K., 1961.
- (39) Schmidt-Rohr, K.; Spiess, H. W. *Multidimensional Solid-State NMR and Polymers*; Academic Press: London, 1994.
- (40) Beckham, H. W.; Spiess, H. W. *NMR: Basic Princ. Prog.* **1994**, *32*, 163–209.
- (41) Batchelder, L. S.; Niu, C. H.; Torchia, D. A. *J. Am. Chem. Soc.* **1983**, *105*, 2228–2231.
- (42) Beshah, K.; Griffin, R. G. *J. Magn. Reson.* **1989**, *84*, 268–274.
- (43) Hiyama, Y.; Roy, S.; Guo, K.; Butler, L. G.; Torchia, D. A. *J. Am. Chem. Soc.* **1987**, *109*, 2525–2526.
- (44) Wann, M. H.; Harbison, G. S. *J. Chem. Phys.* **1994**, *101*, 231–237.
- (45) Forsyth, M.; Meakin, P.; MacFarlane, D. R.; Hill, A. J. *J. Phys.: Condens. Matter* **1995**, *7*, 7601–7617.
- (46) Tracht, U.; Wilhelm, M.; Heuer, A.; Feng, H.; Schmidt-Rohr, K.; Spiess, H. W. *Phys. Rev. Lett.* **1998**, *81*, 2727–2730.
- (47) Floudas, G.; Fytas, G.; Fischer, E. W. *Macromolecules* **1991**, *24*, 1955–1961.
- (48) Jenckel, E.; Heusch, R. *Kolloid-Zeitschrift* **1953**, *130*, 89–105.
- (49) Dubault, A.; Bokobza, L.; Gandin, E.; Halary, J. L. *Polym. Int.* **2003**, *52*, 1108–1118.
- (50) Kuebler, S. C.; Schaefer, D. J.; Boeffel, C.; Pawelzik, U.; Spiess, H. W. *Macromolecules* **1997**, *30*, 6597–6609.
- (51) McCall, D. W. *Acc. Chem. Res.* **1971**, *4*, 223–232.
- (52) Chartoff, R. P.; Weissman, P. T.; Sircar, A. In *Assignment of the Glass Transition*; Seyler, R. J., Ed.; ASTM: Philadelphia, PA, 1994; pp 88–107.
- (53) Sasabe, H.; Moynihan, C. T. *J. Polym. Sci., Part B: Polym. Phys.* **1978**, *16*, 1447–1457.
- (54) Williams, M. L.; Ferry, J. D. *J. Colloid Sci.* **1954**, *9*, 479–492.
- (55) Ferry, J. D. *Viscoelastic Properties of Polymers*, 3rd ed.; Wiley: New York, 1980.
- (56) Royal, J. S.; Torkelson, J. M. *Macromolecules* **1992**, *25*, 1705–1710.
- (57) Victor, J. G.; Torkelson, J. M. *Macromolecules* **1988**, *21*, 3490–3497.
- (58) Smith, P. B.; Moll, D. J. *Macromolecules* **1990**, *23*, 3250–3256.

MA801535D